and those of Taylor *et al.* (*6*) could be due to greater antigenic stimulation of the hosts in our studies as a result of our using highly irradiated cercariae. Other biological or technical factors might also account for the differences; for example, baboon age, sex, and species, schistosome strain, cercarial handling, time of shedding, water *p*H, or temperature.

Figure 4 shows that in the mice, two immunizations produced greater protection than either immunization alone. This supports the findings of Villella *et al.* (*1*), Erickson and Caldwell (*3*), and Hsu *et al.* (*15*) with other experimental hosts. Further work is necessary to establish the optimum irradiation attenuating dose, number of immunizing cercariae or schistosomules, number of immunizations, and interval between immunizations.

M. STEK, JR.*
P. MINARD
D. A. DEAN
J. E. HALL

U.S. Naval Medical Research Institute, Bethesda, Maryland 20014

References and Notes

1. J. B. Villella, H. J. Gomberg, S. E. Gould, *Science* **134**, 1073 (1961).
2. H. F. Hsu, S. Y. L. Hsu, J. W. Osborne, *Nature (London)* **194**, 98 (1962); S. R. Smithers, *ibid.*, p. 1146; J. B. Villella, H. J. Gomberg, S. E. Gould, *J. Parasitol.* **48** (Sect. 2), 19 (1962); A. Perlawagora Szumlewicz and J. C. Olivier, *Science* **140**, 411 (1963); M. G. Radke and E. H. Sadun, *Exp. Parasitol.* **13**, 134 (1963); F. G. von Lichtenberg and E. H. Sadun, *ibid.*, p. 256; E. H. Sadun, J. I. Bruce, P. B. Macomber, *Am. J. Trop. Med. Hyg.* **13**, 548 (1964); A. Perlawagora Szumlewicz, *Bull. WHO* **30**, 401 (1964); H. F. Hsu, S. Y. L. Hsu, J. W. Osborne, *Nature (London)* **206**, 1338 (1965).
3. D. G. Erickson and W. L. Caldwell, *Am. J. Trop. Med. Hyg.* **14**, 566 (1965).
4. S. Y. L. Hsu, H. F. Hsu, J. W. Osborne, *Proc. Soc. Exp. Biol. Med.* **131**, 1146 (1969); S. Y. L. Hsu, *Trans. R. Soc. Trop. Med. Hyg.* **64**, 597 (1970); K. S. Warren and E. O. Domingo, *Exp. Parasitol.* **27**, 60 (1970); S. Y. L. Hsu, G. L. Lust, H. F. Hsu, *Proc. Soc. Exp. Biol. Med.* **136**, 727 (1971).
5. P. Minard, D. A. Dean, R. H. Jacobson, W. E. Vannier, K. D. Murrell, *Am. J. Trop. Med. Hyg.* **27**, 76 (1978).
6. M. G. Taylor, E. R. James, G. S. Nelson, Q. Bickle, B. J. Anderson, A. R. Dobinson, G. Webbe, *J. Helminthol.* **50**, 215 (1976).
7. J. H. Miller, *Trans. R. Soc. Trop. Med. Hyg.* **54**, 44 (1960); G. S. Nelson, *ibid.*, p. 301; E. H. Sadun, F. G. von Lichtenberg, J. I. Bruce, *Am. J. Trop. Med. Hyg.* **15**, 705 (1966); A. Fenwick, *Trans. R. Soc. Trop. Med. Hyg.* **63**, 557 (1969); M. G. Taylor, G. S. Nelson, M. Smith, B. J. Andrews, *Bull. WHO* **49**, 57 (1973); *J. Helminthol.* **47**, 455 (1973); G. Webbe and C. James, *Trans. R. Soc. Med. Hyg.* **67**, 151 (1973); A. E. Butterworth, R. F. Sturrock, V. Houba, R. Taylor, *Clin. Exp. Immunol.* **25**, 95 (1976).
8. D. R. Bell, *Bull. WHO* **29**, 525 (1963).
9. For the screening tests we used enzyme-linked immune sorbent assays [A. Voller, A. Bartlett, D. E. Bidwell, *Trans. R. Soc. Trop. Med. Hyg.* **70**, 98 (1976)].
10. Attenuation was accomplished by exposing the cercariae, contained in 50-ml plastic tubes with aged tap water, to gamma irradiation at 2 krad/min for a total of 60 krad from a bilateral cobalt-60 source at the Armed Forces Radiobiological Research Institute, Bethesda, Md.
11. Citrated saline perfusion fluid was administered by peristaltic pump via a cannula inserted into the descending aorta. Two cannulas inserted superiorly and inferiorly in the hepatic portal vein permitted egress of the perfusate containing the worms.
12. T. K. Yolles, D. V. Moore, D. L. DeGiusti, C. A. Ripsom, H. E. Meleney, *J. Parasitol.* **33**, 419 (1947).
13. K. D. Murrell, S. S. Clark, D. A. Dean, W. E. Vannier, *Exp. Parasitol.* **48**, 415 (1979).
14. H. O. Bushara, M. F. Hussein, A. M. Saad, M. G. Taylor, J. D. Dargie, T. F. De C. Marshall, G. S. Nelson, *Parasitology* **77**, 303 (1978).
15. H. F. Hsu, S. Y. L. Hsu, L. I. Eveland, *Chinese Med. J.* **93**, 297 (1980).
16. We are indebted to J. Rogers for advice on perfusion design and histologic preparations, W. E. Vannier for helpful discussions, and R. C. Salas, H. J. Williams, R. S. Baker, and F. Lyons for technical assistance. This work was supported by the Naval Medical Research and Development Command, Work Unit No. M0095.PN.002.

* Present address: Department of Preventive Medicine and Biometrics, Uniformed Services University of the Health Sciences, Bethesda, Md. 20014.

5 December 1980; revised 26 February 1981

Motility Assay of Human Sperm by Photon Correlation Spectroscopy

Abstract. *Microscopic methods of performing motility assays of spermatozoa are slow, subjective, and involve a small number of spermatozoa. Laser light-scattering methods can analyze the motility of many spermatozoa within minutes. The swimming speed distribution of human spermatozoa was investigated by photon correlation spectroscopy. The sperm was diluted in seminal plasma to avoid modifying the viscosity. The swimming speed distribution was reconstructed from the correlation data by Stock's method of splines. When compared with a videomicroscopic assay, the reconstructed swimming speed distribution accurately reflects translational motion between 0 and 80 micrometers per second, while for speeds greater than 80 micrometers per second the distribution is distorted by the effects of rotational motion.*

Sperm motility has been recognized as a significant factor in reproductive biology since MacLeod and Gold (*1*) established that the forward motion of sperm is the most important single factor in fertilization. Although sperm motility assays are of great importance both in clinical investigations of human fertility and in the practice of animal husbandry, traditional motility assay techniques are far from ideal. Visual microscopic assays can only quantify the movement of a small number of individual spermatozoa and include uncontrollable subjective errors. Microcinematography, while far more precise, is a slow and costly procedure.

Bergé *et al.* (*2*) observed that when laser light is scattered by sperm, the spectrum of the scattered light is dramatically modified by the Doppler shifts produced by motility. Bergé's group subsequently established an experimental clinical program for the study of human motility in collaboration with David and co-workers at the Bicetre Medical Center in Paris (*3*), using this technique of "light beating spectroscopy."

A second approach to motility assays based on laser scattering was initiated by Nossal and Chen (*4*) in a study of *Escherichia coli*. By using photon correlation spectroscopy, which is a fully digital technique, they opened the way for development of a rapid computer-based motility assay which could, in principle, be adapted to routine high-speed precise motility assays.

Nossal and Chen's procedure suffered from two difficulties: (i) wobbling and rotational motion of the swimming organisms distort the data and lead to overestimation of swimming speeds, particularly at large scattering angles, and (ii) the analytic procedure of Fourier inversion used to extract the swimming speed distribution $P(V)$ from the reduced correlation data $g^{(1)}(\tau)$ is highly sensitive both to noise and to the limited delay time span of the data. Subsequently, Stock and Carlson (*5*) showed that difficulties due to wobbling motion could be

Table 1. Results of human sperm motility assays.

Reference	Mean speed, V (μm/sec)	Motile fraction, α
This report:		
Splines analysis	75	0.36
Restricted splines (0 to 150 μm/sec)	57	
Videomicroscopy	46	
Gamma distribution fit (Eq. 1)	65	
Finsey *et al.* (*8*) (range, 0 to 250 μm/sec)	130	
Jouannet *et al.* (*3*) (range, 20 to 180 μm/sec)	96	0.47

0036-8075/81/0626-1520$00.50/0

minimized by working at sufficiently small scattering angles that the scattered intensity becomes essentially independent of orientation. Photon correlation studies of sperm motility have also been reported by other groups (*6*). Shimizu and Matsumoto (*7*) studied pig and abalone spermatozoa by the Fourier inversion procedure of Nossal and Chen. Finsey *et al.* (*8*) fit data obtained with human sperm to the model distribution first advanced by Jouannet *et al.* (*3*)

$$P(V) = (4V/\langle V\rangle^2)\exp(-2V/\langle V\rangle) \quad (1)$$

and Craig *et al.* (*9*) studied the correlation data for bull sperm, taking into account both rotational and translational effects.

We report here a study of human sperm motility including two major innovations (*10*). First, we used a data analysis technique based on the method of linear splines to reconstruct $P(V)$. This approach was developed by Stock (*11*), who successfully applied it to the motile bacterium *Salmonella*. Second, we used a new sample preparation technique that reduces the sperm concentration sufficiently to eliminate multiple scattering while avoiding dilution with aqueous media such as Ringer solution, which modifies the motility by reducing the viscosity of the medium.

Our experiments were performed with a standard photon correlation spectrometer consisting of an argon ion laser, a temperature-controlled (37.5°C) thermostat bath for the 1 by 1 cm sample cuvette, a fast photomultiplier, and a 60-channel digital autocorrelator (*10*). Each sperm sample, freshly produced by a single donor, was collected as two split fractions. The first third of the partitioned ejaculate, which contains 75 percent of the motile spermatozoa, was used to provide the active sample (*12*). The remainder was centrifuged at 48,000*g* for 20 minutes at 37.5°C; the clear plasma was then removed and placed in the sample cuvette. Finally, a small amount of sperm was withdrawn from the active sample with a pipette, which was then inserted into the cuvette and agitated slightly so that the sperm mixed with the clear seminal plasma. This procedure yielded a final concentration of approximately 10^7 spermatozoa per milliliter. The cuvette was then placed in the thermostat bath and allowed to equilibrate for 20 minutes. The total time between ejaculation and the first experimental run was typically 45 to 60 minutes.

Photon correlation functions $g^{(2)}(\tau)$ were obtained at a scattering angle $\theta = 11.82°$ in about 5 minutes. Data were

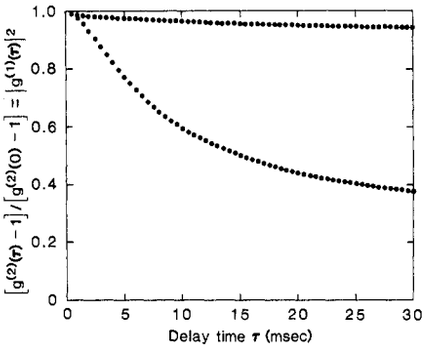

Fig. 1. Intensity correlation function of human spermatozoa diluted in seminal plasma; $T = 37.5°C$, scattering angle $\theta = 11.817°$. (Lower curve) Motile sperm 1 hour after ejaculation; (upper curve) sperm killed by heating.

not collected at any other angles. A typical correlation function for a fresh sperm sample is shown in Fig. 1 (lower curve). A second correlation function was obtained after the sperm were killed by heating, and exhibits the expected translational diffusion of Brownian motion (upper curve).

The measured correlation function $g^{(2)}(\tau)$ is related to the electric field correlation function $g^{(1)}(\tau)$ by

$$g^{(2)}(\tau) = 1 + a|g^{(1)}(\tau)|^2 \quad (2)$$

where a is a geometric quantity ≤ 1 determined by the apparatus. Nossal and Chen (*4*) showed that for an ensemble of point scatterers swimming with an isotropic swimming speed distribution $P(V)$

$$g^{(1)}(\tau) = \int_0^\infty P(V)\frac{\sin qV\tau}{qV\tau}dV \quad (3)$$

where q is the scattering vector [$q = (4\pi n/\lambda)\sin\theta/2$], θ is the scattering angle, n is the refractive index, and λ is the vacuum wavelength of the incident light (488 nm in our experiments).

The effects of nonmotile cells and of diffusion can be included in Eq. 3 in two different ways. Either it can be assumed, as did Stock (*11*), that both the motile and nonmotile cells are diffusing with the same diffusion constant

$$g^{(1)}(\tau) = e^{-Dq^2\tau}[\alpha\int P(V)\frac{\sin qV\tau}{qV\tau}dV + (1-\alpha)] \quad (4)$$

(α is the motile fraction and D is the diffusion constant), or it can be assumed that only the nonmotile cells are diffusing

$$g^{(1)}(\tau) = \alpha\int P(V)\frac{\sin qV\tau}{qV\tau}dV + (1-\alpha)e^{-Dq^2\tau} \quad (5)$$

When used in the data analysis, Eqs. 4 and 5 gave indistinguishable results. Analysis of $g^{(2)}(\tau)$ for entirely nonmotile samples (Fig. 1) by Eqs. 2 and 4 gave $D = 2.7 \times 10^{-9}$ cm^2/sec, equivalent to the translational diffusion constant of a 3-μm-diameter sphere (the dimensions of the sperm head are 2 by 2 by 4 μm).

In Stock's method of splines (*11*), the range of swimming speeds V is divided into N intervals and $P(V)$ is approximated by a series of straight lines joining successive pairs of the $N + 1$ "knots" $P(V_N)$. The integral in Eq. 4 is then evaluated to give a sum of simple functions

$$\int \frac{P(V)\sin qV\tau}{qV\tau}dV = \sum_N P(V_N)C_N(q,V_N,V_{N+1}) \quad (6)$$

The $N + 1$ values of $P(V_N)$ and α are treated as parameters and are varied by a computer program until the result Eq. 4, converted to a theoretical $g^{(2)}(\tau)$ through Eq. 2, gives the best fit to the experimental data.

We also analyzed our data by fitting them to the one-parameter gamma distribution (Eq. 1) following Jouannet *et al.* (*3*). Finally, we carried out a microscopic assay with a television camera mounted on the microscope and a videotape recorder. Samples were prepared exactly

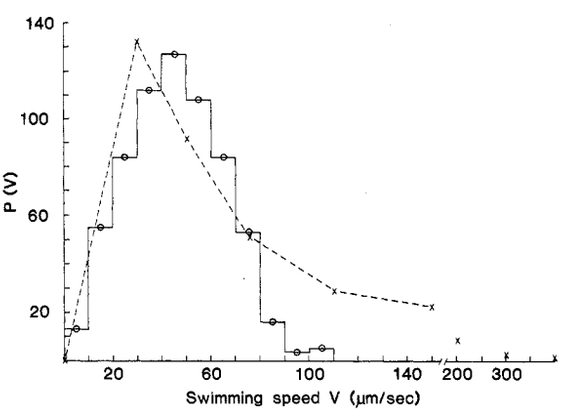

Fig. 2. Swimming speed distribution $P(V)$ found by (x) splines analysis of the data of Fig. 1 and (○) videomicroscopic assay.

as for light-scattering experiments and the assay was performed in a temperature-controlled room at 37.5°C. The videotape was later analyzed to find the swimming speeds of 563 separate spermatozoa, from which a separate swimming speed distribution was constructed.

In performing the splines analysis, the optimum number of parameters $[P(V_N)]$ was selected by minimizing the error $\chi^2 = [g^{(2)}(\tau)_{exp} - g^{(2)}(\tau)_{theor}]^2$. The results of the splines analysis of the data of Fig. 1 are shown in Fig. 2 along with the results of the videomicroscopic assay. Figure 2 shows that for speeds in the range 0 to 80 μm/sec, the splines and videomicroscopic assays agree rather well. However, the "high-speed tail" extending out to speeds well beyond 150 μm/sec is apparently not associated with the translational motion. A plausible explanation for this is that the rotational effects cannot be completely neglected, and their contributions are evident in the high-speed portions of the distribution curve. Craig *et al.* (*9*) state that at a scattering angle of 15°, the electric field correlation function for the large disk-shaped heads of bull spermatozoa (1 by 5 by 9 μm) is dependent entirely on the rotational motion of the head. The head of the human sperm is less anisotropic (2 by 2 by 4 μm) and its correlation data should reflect a mixture of rotational and translational motion. In Table 1 we give the numerical results of our analysis, together with the results of other investigators.

In conclusion, we suggest that photon correlation spectroscopy can provide a fast, reasonably accurate means of establishing the swimming speed distribution of motile sperm through on-line computer analysis utilizing the method of splines. Samples prepared by dilution in seminal plasma circumvent problems associated with multiple scattering while avoiding the reduction of viscosity due to dilution with aqueous media that leads to increased wobbling and distorted swimming speed distributions.

JAMES FROST
H. Z. CUMMINS
Department of Physics,
City College, City University
of New York, New York 10031

References and Notes

1. J. MacLeod and R. Z. Gold, *Fertil. Steril.* **2**, 187 (1951); *ibid.* **4**, 10 (1953).
2. P. Bergé, B. Volochine, B. Billard, A. Hamelin, *C. R. Acad. Sci. Ser. D.* **265**, 889 (1967).
3. M. Dubois, P. Jouannet, P. Bergé, B. Volochine, C. Serres, G. David, *Ann. Phys. Biol. Med.* **9**, 19 (1975); *Nature (London)* **252**, 711 (1974); P. Jouannet, B. Volochine, P. Deguent, C. Serres, G. David, *Andrologia* **9**, 36 (1977).
4. R. Nossal, *Biophys. J.* **11**, 341 (1971); _____, S. H. Chen, C. C. Lai, *Opt. Commun.* **4**, 35 (1971); R. Nossal and S. H. Chen, *J. Phys. (Paris)* **33C1**, 173 (1972); *Opt. Commun.* **5**, 117 (1972).
5. G. B. Stock and F. D. Carlson, in *Swimming and Flying in Nature*, T. Y. Wu, C. J. Brokaw, C. Brenan, Eds. (Plenum, New York, 1975), pp. 57–68. See also M. Holz and S. H. Chen, *Appl. Opt.* **17**, 3197 (1978); J. P. Boon, R. Nossal, S. H. Chen, *Biophys. J.* **14**, 847 (1974).
6. A review of work through 1976 is given in H. Z. Cummins and E. R. Pike, Eds., *Photon Correlation Spectroscopy and Velocimetry* (Plenum, New York, 1977), p. 200.
7. H. Shimizu and G. Matsumoto, *Opt. Commun.* **16**, 197 (1976); *IEEE Trans. Biomed. Eng.* **24**, 153 (1977).
8. R. Finsey, J. Peetermans, H. Lekkerkerker, *Biophys. J.* **27**, 187 (1979).
9. T. Craig, F. R. Hallett, B. Nickel, *ibid.* **28**, 457 (1979).
10. J. Frost, thesis, New York University (1977).
11. G. B. Stock, *Biophys. J.* **16**, 535 (1976); thesis, Johns Hopkins University (1977).
12. E. Tyler and H. Singher, *J. Am. Med. Assoc.* **160**, 94 (1956).
13. We thank G. Stock and F. Carlson of the Department of Biophysics of Johns Hopkins University for furnishing the computer program used in the splines analysis and for many helpful discussions. We also thank J. Oscinchak and J. Downey of the Department of Biology of City College for their help and the use of their equipment in performing the videomicroscopic assays. Finally, we wish to acknowledge several helpful conversations with P. Bergé, B. Volochine, J. P. Boon, and S. D. Cosloy.

26 December 1979; revised 18 November 1980

Remodeling of Multiterminal Innervation by Nerve Terminal Sprouting in an Identifiable Lobster Motoneuron

Abstract. *A single motoneuron provides multiterminal innervation to the limb accessory flexor muscle in lobster. Its nerve terminals and synapses relocate to more distal sites during primary development and growth beyond sexual maturity. This remodeling of multiterminal innervation occurs by sprouting of nerve terminals and synapses from preexisting ones.*

The development of innervation occurs by the sprouting of intact axons at their peripheral fields (*1*). Although such sprouting has been found largely during primary development, there is evidence that it occurs in mature stages as well, where it may replace old nerve terminals (*2, 3*). This raises the intriguing possibility that nerve terminals in the periphery and the central nervous system (CNS) are in a dynamic state because of constant growth and restructuring by the sprouting mechanism. We have found a remodeling of the multiterminal innervation arising from a single identifiable lobster motoneuron during primary development. It consists of a shift in nerve terminals and synapses to the ever more distal and finer branches of the axon by sprouting from preexisting terminals and synapses. Such sprouting also occurs in several sizes of large and chronologically older adult lobsters, which suggests that the restructuring of multiterminal innervation occurs throughout life.

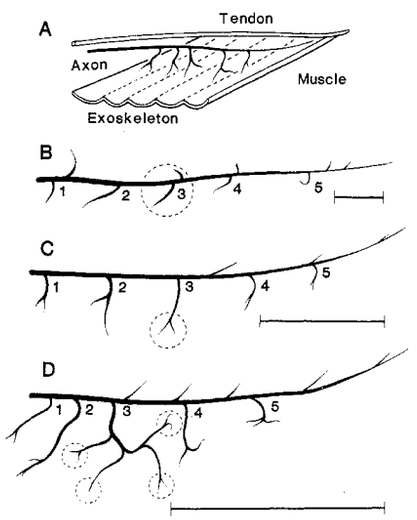

Fig. 1. Location of five primary branches on the exoskeletal side of the single excitor axon to the DAFM in an adult lobster (A) and their development as seen in a 1-day-old (first stage) larva (B), a 1-year-old (twelfth stage) juvenile (C), and a 5- to 7-year-old adult (D). Primary branches are numbered 1 to 5, proximal to distal. Encircled areas show the typical location of nerve terminals and neuromuscular synapses in the comparable branch 3 region of each developmental stage. Scale bars (B) 0.01 mm; (C) 1 mm; and (D) 10 mm.

We studied multiterminal innervation to the accessory flexor muscle in the walking legs of lobster (*Homarus americanus*) because it is supplied by a single excitatory and inhibitory axon (*4*). The branching pattern of the excitor axon can be easily distinguished from that of the inhibitor in preparations stained with methylene blue, as the excitor has a larger diameter (*5*). Furthermore, the nerve terminals of each axon have synaptic vesicles that differ in shape with aldehyde fixation: vesicles of excitatory terminals are spherical, those of inhibitory terminals, ellipsoidal (*6*). These features enabled us to identify the single excitatory neuron to the distal accessory flexor muscle (DAFM) in the first walking leg and to reconstruct its branching pattern by methylene blue staining in juvenile and adult lobsters and by serial section electron microscopy in a larval lobster (*7*). The latter technique was also used to identify and locate nerve terminals and synapses in all of the lobsters examined.

At a gross level, the development of

0036-8075/81/0626-1522$00.50/0